CHAPTER NINE

DISCUSSIONS

LAVES PHASE EMBRITTLEMENT

9.1 INTRODUCTION

In this chapter the parameters that affect embrittlement of the type 441 ferritic stainless steel are discussed. Parameters such as the grain size, grain boundary Laves phase and the cooling rate were tested against existing fracture theories of Stroh, Cottrell and Smith. Also, the effect of possible niobium solute drag during the recrystallisation and grain growth was considered qualitatively.

9.2 PRECIPITATES FOUND IN AISI 441 FERRITIC STAINLESS STEEL

Thermo-Calc® calculations predict that the phases that are stable over a wide range of temperatures in these steels are the Laves phase, carbo–nitrides and the sigma phase in a structure that remains completely ferritic from its initial solidification. The presence of the M_6C or (Fe_3Nb_3C) type carbides were detected experimentally using XRD and TEM analyses. But this precipitate seems to appear infrequently in these steels and its volume fraction could not be quantified due to its low value. In the TEM image they appear as coarse grain boundary precipitates, see Figure 9.1. Such coarse precipitates are known not to cause any significant strength after high temperature ageing [5]. But the presence of the coarse M_6C type carbides can be prevented by adding elements which have a stronger affinity for carbon than the Nb in these steels, that is Ti. The amount of Nb addition depends on the carbon and nitrogen content, and it was found that an addition of 0.1wt.%Ti is normally enough to stabilise 0.02 wt.%C and N as Ti(C,N) [5].

Angular carbo-nitrides of titanium and niobium that have precipitated from or soon after the melt are randomly dispersed throughout the structure. The presences of these second phases in these steels tend to lower the melting point of the steel [55]. Excess niobium is taken into solid solution during high temperature annealing and is re-precipitated as very fine particles of the Laves phase (Fe_2Nb) upon either slow cooling or upon holding at intermediate temperatures of 600 – 950 °C [136]. Strengthening by

this dispersion was found to be responsible for improved elevated temperature strength [8,69]. Although Thermo-Calc® calculations show the presence of the sigma phase as an equilibrium phase, others have indicated that this phase is not supposed to form in this type of alloy and neither was it encountered in this study. It has often been reported that sigma phase precipitates in high chromium ferritic stainless steels but only after very long periods at high service temperatures [25,26,27].

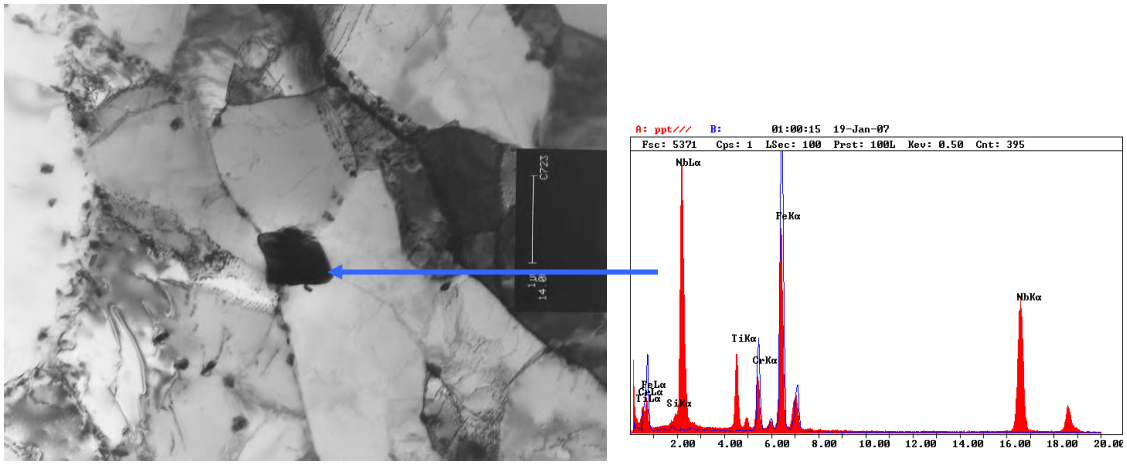

Figure 9.1. TEM micrograph shows the presence of the M_6C or (Fe_3Nb_3C) type carbide in the subgrain structure from Steel A. Note that the specimen was annealed at 700 °C for 30 minutes and other fine particles were determined to be Fe_2Nb Laves phase particles.

9.2.1 Effect of the Steel's Composition on the Precipitate's Solvus Temperature

The solvus temperature and volume fraction for each phase is alloy composition dependent. From the Figures 5.4 to 5.8 in Chapter 5; the minimum temperature for the dissolution of the Laves phase and the carbonitrides were estimated. These dissolution temperatures for the Laves phase were used as a guide to avoid excessive grain growth during higher annealing temperatures. Using Steel A with a nominal composition of 0.012C-0.0085N-0.444Nb-0.153Ti-~0Mo as this study's reference steel, it was established that the C and N contents have a significant impact on both the solvus temperature and composition of the (Ti,Nb)(C,N), with increasing one or both of them resulting in increments of both solvus temperature and volume fraction.

The Laves phase's formation was found to be more dependent on the Nb content than on the Ti content. Decreasing the Nb content of the steel, decreased both the solvus temperature and volume fraction of the Laves phase. For instance, by reducing the Nb content to 0.36wt % in Steel C (0.023C-0.024N-0.36Nb-0.171Ti-<0.01Mo) as compared to 0.444wt % in Steel A, this resulted in lowering the solvus temperature to 765 °C (as

compared to 825 °C in Steel A) and the weight fraction determined at 600 °C was reduced to 0.573 wt% (compared to 0.92 wt% in Steel A). An increase in Ti content in Steel C, to 0.171 wt% (compared to 0.153 wt % Ti in Steel A) did not have any significant impact on the both solvus temperature and weight fraction of the Laves phase. A Mo addition was found to increase the volume fraction of the Laves phase, whilst at the same time lowering its solvus temperature. For instance, it has been observed in this study that a Mo addition from practically zero in Steel A to 1.94 wt % in Steel E enhanced the formation of the Laves phase in the Nb-Ti-Mo steel (see Figure 5.8 and Table 5.6), while at the same time slowing its precipitation kinetics (see Figure 8.5). Some authors have observed that this is due to the Mo retarding the diffusivity of Nb to form Laves phase precipitates [5,6,135]. A more detailed analysis of the kinetics of nucleation of the Laves and other second phases in this and other similar Nb-containing ferritic stainless steels will be reported in Chapter 10.

The Thermo-Calc® results of Steel A where compared with the experimental results of obtained from the XRD analysis, see Figure 9.2. The results from Thermo-Calc® predict that at 825 °C, the weight fraction of the Laves phase should be zero, whereas the experimental results found that there was still about 0.031wt% present and a further remnant still existed even at 850 °C and above. The presence of the Laves phase up to a temperature of 950 °C in a similar ferritic stainless steel to the one studied in this work, was observed by other researchers, where they have observed that the Laves phase improved the high temperature strength of their steel [69,136].

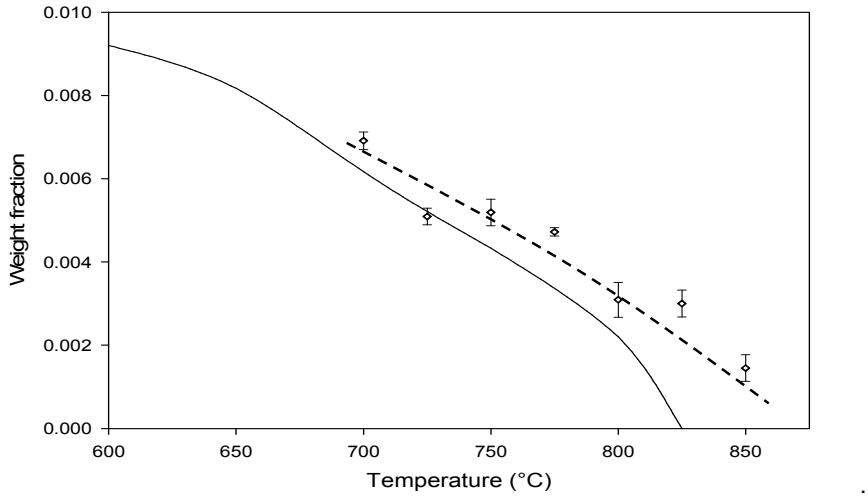

Figure 9.2. Comparison between experimental and Thermo-Calc® calculated weight fractions of Laves phase in Steel A. The points and dotted line represent the experimental results while the full line is as predicted by Thermo-Calc® for this steel.

9.2.2 Effect of the Steel's Composition on the Precipitate's Composition

It was established from the Thermo-Calc® predictions that the composition of the titanium and niobium carbonitrides (Ti,Nb)(C,N) is not affected by a change in the steel's composition, but only the stoichiometric composition is affected. On the other hand, the Laves phase's composition is highly affected by the change in the steel's composition. Thermo-Calc® predictions show that the composition of the Laves phase in Steels A and B contains the following elements: Fe, Cr, Ti and Nb, but no C or N, and this led to the conclusion that the Laves phase is in the form of $(Fe,Cr)_2(Nb,Ti)$. The absence of C or N in the Laves phase was also observed by Sawatani et al. [8], using an electron probe microanalysis technique, but in the work of Lundin [137] on a 10.6Cr-1.01W-1.02Mo-0.04Nb ferritic stainless steel and using an atom-probe field-ion microscopy (APFIM) analysis of the Laves phase, the author found carbon to be soluble in the Laves phase. It needs to be noted, however, that the respective carbon contents of the two steels from the work by Sawatani [8] and Lundin [137] were 0.008%wt. and 0.11%wt, respectively. Therefore, the solubility of the carbon in the Laves phase appears to be directly dependent on the carbon content of the steel.

When the Nb content is reduced and the Ti content is increased (as in the Steel C (0.36Nb-0.171Ti)) or only the Ti is decreased (as in Steel E (0.251Nb-0.106Ti)), Thermo-Calc® predictions show that Ti is not taken up into the Laves phase, but resulted in an increase in the Ti-content of the Ti(C,N) in this steel. The discrepancy caused by the Ti solubility in these alloys as compared to other alloys could not be established from this work. Therefore, a further study to gain a better understanding on the solubility of Ti in the Laves phase in these steels is needed.

In the case where Mo additions were made, such as in Steels D and E, it was found that Mo is taken up into the Laves phase as $((Fe,Cr)_2(Nb,Ti,Mo)$ for Steel D and $(Fe,Cr)_2(Nb,Mo)$ for Steel E respectively. It was, therefore, concluded that the nominal composition of the Laves phase should be reported according to the major alloying elements, i.e. for Steels A – D as Fe_2Nb and for Steel E as $Fe_2(Nb,Mo)$ respectively.

9.3 EMBRITTLEMENT OF TYPE 441 FERRITIC STAINLESS STEEL

9.3.1 EFFECT OF GRAIN SIZE ON FLOW STRESS: THE HALL-PETCH RELATIONSHIP

The change in grain size of Steel A was introduced by annealing the as received and plant-embrittled material at temperatures of 850 to 1100 °C, i.e. above the estimated Laves phase solvus temperature. From Section 6.3.4 in Chapter 6, the results show a steady increase in grain size up to about 950 °C, but between 950 °C and 1000 °C there is a sudden and rapid 60 % increase in the mean linear intercept grain size. When the effect of the grain growth on the 0.2% yield strength in this steel was tested according to the Hall-Petch relationship, it was found that it only applies in the temperature range of 850 °C to 950 °C (see Figure 9.3) but beyond 950 °C, the relationship did not hold. The Hall – Petch relationship is given by:

$$\sigma_y = \sigma_0 + k_y^s d^{-\frac{1}{2}} \qquad \text{Equation 9.1}$$

where σ_0 is the friction stress due to dislocation obstacles on the slip plane in the materials, k_y^s is the locking parameter representing the grain boundary as an obstacle to propagation of deformation, and d is the grain size. According this Equation 9.1, plastic deformation leads to a pile-up of dislocations at the head of a slip plane at a grain boundary. This pile-up causes stress concentrations at the boundary and in the adjacent grain. When the stress concentration is high enough and reaches a critical value, a dislocation source in the adjacent grain may be activated and plastic deformation can spread out into this next grain. The values for σ_0 and k_y^s in this material were determined experimentally as 229.03 MPa and 469.8 MPa .$\mu m^{1/2}$, respectively from Figure 9.2, although the relatively few data points and their scatter (see the relatively low value of the regression coefficient R^2) make these values somewhat approximate. In the work by Miyahara et al. [138], working on two types of ferritic steels with a fine and coarse grain size, the authors have estimated a locking parameter of 260.0 MPa .$\mu m^{1/2}$ which was in good agreement with the conventional results for a low – carbon steel from Pickering's [47].

Comparing this value with the value obtained from this work, it can be concluded that grain boundary strengthening at temperatures ranging up to 950 °C was sufficient to prevent the embrittlement of this steel and, therefore, the source of embrittlement found in this study is most likely from the presence of the Laves phase precipitates on sub- and grain boundaries.

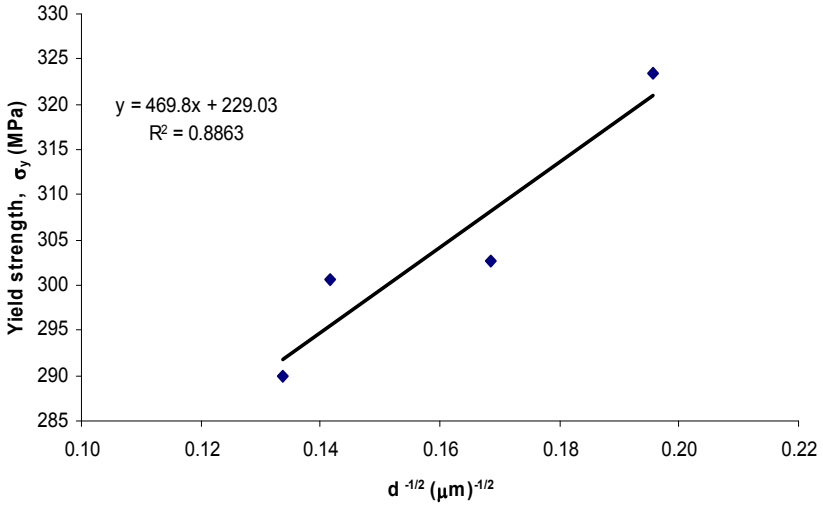

Figure 9.3. The effect of grain size on the yield strength of Steel A.

9.3.2 CRACK NUCLEATION

According to Stroh [36], the value for the shear stress created by a dislocation pile – up of length $d/2$ to nucleate a microcrack is as follows:

$$\tau_e \geq \left[\frac{\pi G_m \gamma_f}{2(1-\nu)d}\right]^{\frac{1}{2}} \qquad \text{Equation 9.2}$$

where τ_e is the effective shear stress; γ_f is the effective surface energy of the crack; G_m is the shear modulus; ν is Poisson's ratio; d is the grain size. The shear stresses are comparable for the constant $G_m b/\gamma_f \sim 8$ [36], where b is the Burgers vector of the slip plane. Assuming that $G_m b/\gamma_f \approx 8$, with $G_m = 8.6 \times 10^{10}$ Pa and $b = 2.48 \times 10^{-10}$ m, then $\gamma_f \approx 2.67$ J/m^2. It should be noted that this estimated effective surface energy of the crack is much higher than that of the grain boundary energy in stainless steels which is in the region of 0.5 to 0.7 J/m^2 and that for the free surface about three times higher, i.e. about 1.5 to 2.1 J/m^2 [40,139]. According to Cottrell [38], an effective surface energy of the crack greater than the true one appears to be a common feature of brittle fracture in iron which is thought to be mainly due to irreversible work of tearing grain boundaries. For the specimen annealed at 850 °C which had a grain size of 26.1 µm, and with ν = 0.28 and using Equation 9.2, produces an estimate of the effective shear stress of approximately 438 MPa. This value is significantly higher than the measured yield strength of 323.5 MPa for this steel (see Figure 9.4) after annealing at 850 °C, leading to a conclusion of ductile and not brittle failure at this grain size. From these results, it can

furthermore be concluded that if a crack nucleus can form, any increase in its propagating length can lead to a decrease in the total system's energy, provided that there is no change in the surface energy encountered during the crack growth. The critical number of dislocations that is sufficient to nucleate a crack at the end of the slip-band is given by:

$$n = \frac{\pi^2 \gamma_f}{2\tau_e b} \qquad \text{Equation 9.3}$$

If the steel does show a tendency to fracture in a brittle manner, either because of a low temperature or from brittle precipitates on the grain boundaries, then a smaller grain size d would be helpful. The shear stress at the head of the dislocation pile up is given by $n\tau_e$, *i.e.* the smaller the grain size, the smaller the number of dislocations in the pile-up when the slip band arrives at the grain boundary.

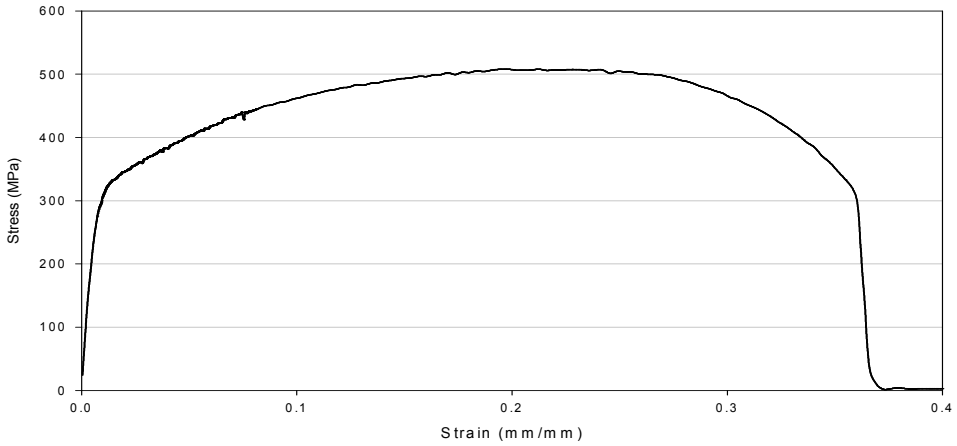

Figure 9.4. A room temperature tensile test of the specimen of Steel A that was annealed at 850 °C for 30 minutes and then water quenched.

When secondary precipitates are inhomogeneously distributed (such as the grain boundary Laves phase precipitates) the value of the surface energy γ_f may be reduced and the amount of work done in nucleating a crack decreases. Thus the crack initiates more easily at grain boundaries, even though the resulting cracks probably propagate transgranularly and not intergranularly. In the present study there is evidence of the (Ti,Nb)(C,N) precipitates that have cracked after Charpy impacting the sample annealed at 850 °C (see Figure 9.5). These carbo-nitride precipitates present on the fracture face were found to be distributed within the grains, and their volume fraction V_v was

relatively much lower compared with that of the Laves phase. In this case, for the given volume fraction of the (Ti,Nb)(C,N) precipitates γ_f will be higher for a distribution within the grain's interior.

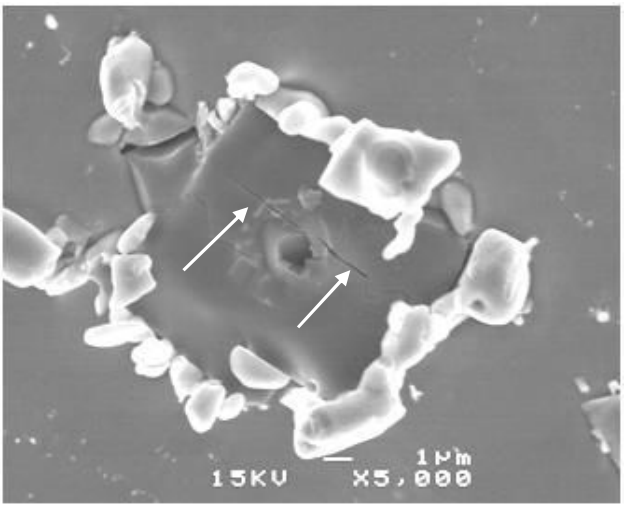

Figure 9.5. High resolution field emission scanning microscope image showing the cracking of (Ti,Nb)(C,N) particles after impact testing the specimen at room temperature. This specimen of Steel A was annealed at 850 °C followed by quenching in water.

The stress causing cleavage fracture is, therefore, predicted to be the effective shear stress:

$$\tau_e = \tau_y - \tau_i = k_y^s d^{-\frac{1}{2}} \qquad \text{Equation 9.4}$$

where τ_y is the shear yield strength and τ_i is the lattice friction stress. If yield occurs at the head of the slip band by nucleation of a crack, it can be assumed that the friction stress for yield is approximately the same as for the dislocations in the piled up slip band [24]. The above Equation 9.4, does not explain why cleavage fracture is predominant in the presence of precipitates (where the yield strength is high, but the $(\tau_y - \tau_i)$ may be little different from its value at room temperature).

9.3.3 Effect of Precipitates in the Embrittlement of this Steel

9.3.3.1 Embrittlement and the Cottrell's Approach

Based on the results of Steel A as shown in Chapter 6, it was observed from Figure 6.12 that the Charpy impact energy values indicate decreasing embrittlement with increasing

annealing temperature up to 850 °C, which correlates with the Thermo – Calc® predictions of a decreasing volume fraction of Laves phase as 825 □C is approached. The same observations where made by Sawatani et al.[8] working on a Ti and Nb stabilised low C, N – 19%Cr – 2%Mo stainless steel whereby they have observed that an increase in the volume fraction of the Laves phase has a significant impact in promoting embrittlement of their steel, but the authors did not make any detailed analysis of why the presence of the Laves phase deteriorates the impact toughness. In the work done by Grubb et al.[140], they have suggested that the embrittling effect arises from the flow stress increase associated with the α' – precipitation (i.e. 475 °C embrittlement) and this can be readily understood using the approach of Cottrell. This approach provided a useful basis for understanding the micromechanics of brittle fracture even though, strictly speaking, the model does not encompass all the practical modes of crack initiation [38]. The conditions for cleavage fracture can be expressed by the Cottrell equation:

$$\sigma_f k_y^s d^{\frac{1}{2}} = C_1 G_M \gamma_f \qquad \text{Equation 9.5}$$

where σ_f is the fracture stress, C_1 is a constant related to the stress (~4/3 for a notched specimen and 4 for a plain specimen [21]), and the rest are as mentioned previously. The ferritic stainless steels generally display a substantial increase in lattice friction stress σ_0, upon rapid cooling. This increase manifests itself in an increase in the ductile to brittle transition temperature (DBTT), in accordance with the Cottrell approach, which predicts that the DBTT or brittle fracture with grain size as a variable, will occur when $\sigma_f = \sigma_y$ which would lead to [18,19]:

$$\sigma_y k_y^s d^{\frac{1}{2}} = k_y^{s\,2} + \sigma_i k_y^s d^{\frac{1}{2}} = C_1 G_M \gamma_f \qquad \text{Equation 9.6}$$

Therefore, if $\sigma_y k_y^s d^{\frac{1}{2}} > C_1 G_M \gamma_f$, then brittle fracture occurs, and if $\sigma_y k_y^s d^{\frac{1}{2}} < C_1 G_M \gamma_f$, then ductile fracture will take place. The yield strength σ_y is related to the grain size through the Hall – Petch equation, that is Equation 9.1. At 850 °C, assuming that the yield strength σ_y = 323.5 MPa, k_y^s is approximately 469.8 MPa .μm$^{1/2}$ and with a grain size of 26.1 μm, it can be seen qualitatively that according to Equation 9.6, this steel will be brittle at the temperatures *above* 850 °C where the grain size increases due to grain growth. However, there is not much of a difference in grain size between the as

received steel and the specimen of Steel A annealed at 850 °C or at lower temperatures. Therefore, it cannot be confidently assumed that at temperatures *below* 850 °C, that the grain size plays a significant role in embrittling this steel.

The presence of large pre-existing cracks is, therefore, not a necessary prerequisite to cause a brittle fracture [43]. It is obvious from Equation 9.6 that grain size has a direct effect on the ductile – to – brittle transition temperature (DBTT). A reasonable relationship expressing the DBTT at which the fracture stress (σ_f) and yield strength (σ_y) are equal for a given grain size d^* has been proposed, i.e. for a given material, there is a theoretical and experimental justification of a relationship between the grain size and transition temperature :

$$DBTT = D + 1/\beta \ln d^{*\frac{1}{2}} \qquad \text{Equation 9.7}$$

where D is a constant and the slope ($1/\beta$) should also be constant. These variations of the DBTT with the grain size that turn out to be consistent with Equation 9.7 have been noted previously by different authors [19,43,141]. The same relationship was tested in the current work, and it was observed that there is a tendency for the DBTT to increase linearly with $\ln d^{*\frac{1}{2}}$ (see Figure 9.6). For AISI type 441 stainless steel studied here, it was observed that over the range of grain sizes from 25.2 to 55.9 µm, there is a shift of 35 °C in the transition temperature. In the work of Plumtree and Gullberg [43] on Fe-25Cr ferritic stainless steels with 0.005 wt%C and 0.15 wt%N, the authors noted a positive shift of 26 °C in a grain size increase of 33 to 95 µm. These authors have also observed that by increasing the interstitial element contents of the steel, this will reduce the sensitivity of the transition temperature to the grain size. This indicates that by changing the composition of the steel and making it less impure (such as with Steel C – E), the dependence of the DBTT to the grain size becomes less sensitive. According to some authors [43,19], they have observed that from a qualitative viewpoint, the effect of grain size on the ferritic stainless steel's transition temperature may be somewhat less than projected by Equation 9.7. But from the current work it was observed that a shift of even 10 °C is significant to be considered when using Equation 9.7.

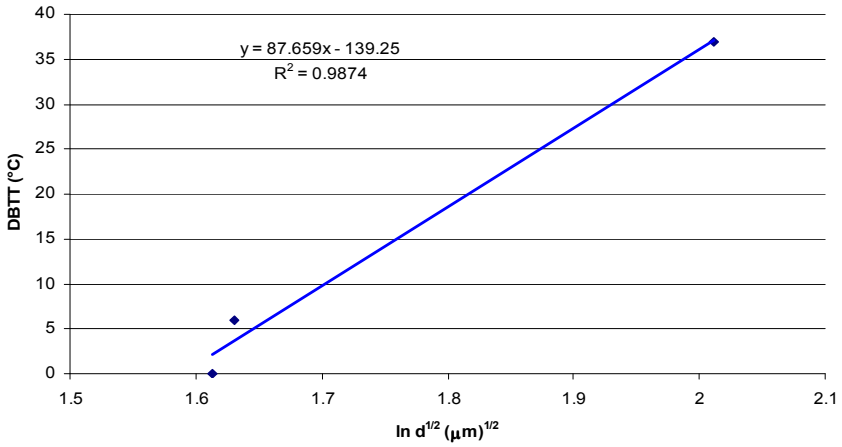

Figure 9.6. The plot of transition temperature versus {ln $d^{1/2}$} of 441 ferritic stainless steel, Steel A.

Generally, the toughness of ferritic stainless steel can be assessed in terms of the DBTT, or a temperature below which Equation 9.6 appears to be satisfied for a given material by the flow stress also being the fracture stress, i.e. brittle fracture without any significant plastic yielding. The satisfaction of Equation 9.6 with decreasing temperature is generally associated with the tendency for the flow stress to increase with decreasing temperature. High strain rates and constraints to plastic flow at the root of a notch have the effect of raising the flow stress and lowering the value of C_1 and thus, promoting satisfaction for Equation 9.6. According to the Cottrell model this phenomenon may be explained by the fact that the locking of dislocations by interstitials in bcc materials causes the flow stress to increase. However, the solubility level of the interstitials carbon and nitrogen in ferritic stainless steel is sufficiently low that it is rarely possible to distinguish between solute embrittling effects and the effect of second-phase precipitates.

9.3.3.2 EMBRITTLEMENT BY GRAIN BOUNDARY PRECIPITATES (THE SMITH'S MODEL)

The precipitates, in fact, become more important than the solute when the amount of interstitial elements significantly exceeds the solubility limit. The presences of interstitials in an amount in excess of the solubility limit, serves to increase the DBTT still further. This embrittling effect is closely linked to the number and size of precipitates formed on the grain boundaries. Thick precipitate films act as strong barriers to slip propagation across the grain boundaries and raise k_y^s . In this case, the Smith approach [39] can be used for a growth controlled cleavage fracture that incorporates a brittle precipitate on grain boundaries. Here a Laves phase particle of thickness C_o at

the grain boundary dividing adjacent grains, is cracked by the dislocation pile – up of length d *(which may be related to the grain size itself).* The important stress in causing fracture is predicted to be the effective shear stress, and it may be analysed in a manner similar to that for the Cottrell model to obtain a failure criterion in the absence of plastic flow by dislocations:

$$\sigma_f > \left[\frac{4E\gamma_f}{\pi(1-\nu^2)C_o}\right]^{\frac{1}{2}} \qquad \text{Equation 9.8}$$

where E is Young's Modulus, σ_f is the fracture stress; γ_f is the effective surface energy of the interface between the ferrite grain and the Laves particle, and ν is Poisson's ratio. Assuming, the earlier estimated effective surface energy of $\gamma_f \approx 2.67$ J/m^2, with G_m = 8.6 x 10^{10} Pa and E = 8/3 G_m = 2.29 x 10^{11} Pa. For the specimen annealed at 850 °C, the largest Laves phase precipitates measured were about 513 nm in thickness. With ν = 0.28 and using Equation 9.8, this gives a fracture stress of approximately 787 MPa. This value is much higher than the experimentally determined yield strength value of 323.5 MPa, once more not predicting brittle fracture to occur. Although not agreeing quantitatively with Smith's model, the above relationship clearly indicates qualitatively that coarser Laves particles with a higher value of C_0 give rise to lower fracture stresses, and also predict that σ_f is independent (directly) of the grain size. However, in practice a fine grain size is often associated with thinner particles due to a higher nucleation rate upon forming the particles, and the value of σ_f is then expected to be higher. Grain boundary Laves phase precipitation can be suppressed by quenching from above the solution temperature when the interstitial content is low. However, the resulting fine intergranular precipitation may increase the DBTT by increasing the lattice friction stress (σ_o). This model appears to explain at least qualitatively the cause of the embrittling effect associated with the Laves phase precipitation in the fracture of AISI type 441 ferritic stainless steel.

In work done by Sim et al.[3] on a Nb stabilised ferritic stainless steel, they have shown that the high temperature strength decreases with increasing ageing time at temperatures between 600 °C and 950 °C, and this was mainly due to the loss of the solid solution hardening effect as the Nb is transferred from the matrix into the Laves phase. They have also observed that the rate of reduction in yield strength as a function of the Nb content at an ageing temperature of 700 °C, showed a linear relationship with the Nb content in solid solution. In their conclusion, they observed that during ageing at 700 °C, Nb(C,N) and Fe_3Nb_3C precipitate out and decrease the high temperature

strength slowly while the precipitation of the Fe_2Nb Laves phase at 700 °C decreases the high temperature strength more abruptly. This is reasoned to be because of the *Lifshitz-Slyosov-Wagner* (LSW) quasi-equilibrium coarsening rate of the Laves phase that appears to be much faster compared to that of Nb(C,N). This was believed to be due to the incoherent high energy interface between the Fe_2Nb and the matrix, with the Fe_2Nb having a higher surface energy than that of Nb(C,N). Thus, it can be concluded that coarse Fe_2Nb precipitates are very detrimental to the high temperature strength of type 441 stainless steels.

In work done by other researchers on ferritic stainless steels it was shown that the tensile strength increases with annealing temperature above 1000 °C whilst the percentage elongation decreases [8]. Therefore, from such an observation it can be postulated that as the annealing temperature increases the amount of niobium in solution also increases due to dissolution of precipitates and this should, therefore, increase the yield strength due to solid solution hardening. But in the present work the same effect was not observed since the yield strength decreased with increasing solution treatment temperature (see Figure 6.16), which is indicative of a grain coarsening effect. Yamamoto et al.[69] have observed in a ferritic steel with composition Fe – 10at.% Cr – Nb with 0.5 – 5 at.%Nb, that it is possible to design a steel strengthened by Fe_2Nb Laves phase to give an excellent high temperature strength. They have suggested that the strength is insensitive to Nb content, but an optimum concentration of about 1 – 1.5 at.% Nb would provide a proper volume fraction of the Laves phase to ensure good room temperature ductility. None of these authors, however, had attempted to make any correlation between the Laves phase volume fraction present and high strain rate testing such as the Charpy impact test. It is of course well known that one may find good strength and even good ductility values at slow strain rate testing without any sign of brittleness and the practicality of strengthening these alloys by Laves phase needs to be approached with caution.

It should be noted that both the fracture and the yield strength depend on the grain size, and refining the grain size will result in an increase of these strengths. According to the above Cottrell model on the DBTT, the effective temperatures for the DBTT from an increased grain size exists when the flow stress practically equals the fracture stress with very little measurable plastic strain. In this case, that will be at 950 °C where there is no grain boundary Laves phase. From Figure 9.7, the grain size increase between 850 and 950 °C is about 1.6 times or a 60% increase. According to Equation 9.1, it can be concluded that by increasing the grain size, both the fracture stress and the flow

stresses will be decreased, and this will certainly shift the DBTT upwards. In work by Kinoshita [42] on 18Cr-2Mo steel and 26Cr–4Mo steel, the author however, found no significant grain size dependence of the DBTT where the grain size was varied through strain annealing. However, many other authors have reported such a relationship as was also found here. In cases where there are grain boundary precipitates present, such as with the specimens annealed below 850 °C, the Laves phase will tend to lower the cleavage fracture stress. In this case a crack nucleus is formed by the separation of the particle–matrix and this interfacial crack initiates transgranular fracture, but that has not been observed to cause grain separation.

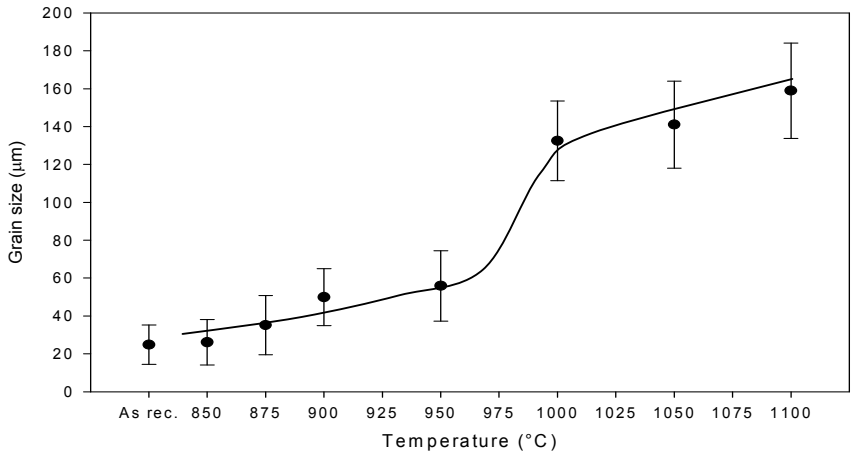

Figure 9.7. Effect of annealing temperature above 850 °C on the grain size for the AISI type 441 stainless steel, Steel A.

9.3.3.3 Effect of Cooling Rate

When the specimens were slowly cooled from the solution treating temperature above the Laves phase solvus temperature, precipitation of the Laves phase occurred afterwards during slow cooling. Steels embrittled from such a treatment behave very similarly to those treated below the solvus temperature [7]. This points to the usefulness of constructing a time – temperature – precipitation (*TTP*) curve for Laves phase formation and such a *TTP* curve was determined experimentally for Steel A and was reported in Chapter 8. Heat treatments that accelerate the precipitation of the Laves phase (that is, below 850 °C) decrease the resistance to crack initiation significantly during dynamic loading. It can be assumed that the volume fraction of the Laves phase, particularly on the sub- and grain boundaries, plays a significant role in affecting both the transition temperature and the upper-shelf energy and that the degree of embrittlement should increase as the volume fraction increases at lower annealing temperatures (see

Figure 5.4), as also predicted by the Smith model of embrittlement by grain boundary phases in ferritic steels. The width C_o (according to Equation 9.8) of the embrittling second phase is related firstly, to the volume fraction V_v of the Laves phase but also secondly, to the grain size, the latter through the grain boundary nucleation site concentration with a larger sub- and grain size leading to a thicker C_0 through less available Laves phase nucleation sites. Therefore, both a higher volume fraction as well as a larger sub- and grain size will then indirectly decrease the effective fracture stress of the steel through a higher value of C_0. This was indeed found in Figure 6.12 with annealing temperatures decreasing from 850 to 600°C, raising the volume fraction of the Laves phase. Other authors have shown that there is an optimum annealing temperature at which the quantity of the Laves phase Fe_2Nb reaches a maximum, and this temperature depends critically on the Nb content in the steel [7,4,99], no doubt through non-equilibrium volume fractions according to a relevant CCT type phase transformation diagram. In the current work reported here, therefore, some remaining Laves phase on grain boundaries at 850°C could have contributed to a lower upper shelf energy if compared to the specimen annealed at 950 °C where dissolution should have been complete.

Further analyses on the specimens that were annealed at 600, 700 and 850 °C, showed from the Thermo-Calc® results (see Figure 5.4), that the predicted weight fraction of the Laves phase at 600 °C is about 0.92 %wt, at 700 °C is about 0.67 %wt and at 800 °C is about 0.14 %wt and that there should be no Laves phase present at 850 °C. Note, however, that Thermo-Calc® only gives an estimated weight fraction at *full equilibrium conditions* and it does not reveal anything about the nucleation rate and the kinetics of the Laves phase formation before equilibrium has been achieved. In the current study as reported in Chapter 8 on the kinetics of the formation of the Laves phase, it was observed that the precipitation kinetics of the Laves phase are much higher at 700 °C than at either 850 °C or 600 °C, and this resulted in a double nose *TTP* curve. From this it follows that at 700 °C after equal times at temperature, the volume fraction of the Laves phase would be much higher than either at 850 or at 600°C and this will result in the specimen having a lower upper shelf energy at 700°C than the specimen annealed at 600 °C.

From the measurement of the DBTT at room temperature and shown in Figure 6.17, which falls within the ductile to brittle transitions but not at the same points for the two temperatures, the specimen annealed at 950 °C is at the very bottom of the transition while at 850 °C it is in the middle. A direct comparison of the absolute values on the two

curves is, therefore, not feasible as they fall within different parts of the transition curve. At 950 °C the grain size effect is overwhelming (even more significant than the effect from the Laves phase) and that the addition of Laves phase to an already brittle steel at slow cooling rates, brings in no measurable further embrittlement. Therefore, the full effect of the Laves phase precipitation on the Charpy impact toughness could be seen only in the specimen annealed at 850 °C where the grain size effect was minimal. Therefore, samples that were solution treated at 850°C show a significant decrease in the impact toughness with decreasing cooling rates that allow Laves phase to form during slow cooling. Specimens that were solution treated at 950 °C, however, show only a slight increase in impact toughness after slow cooling of 10 °C/sec, and then the toughness levels off with a further increase in cooling rate (see Figure 6.18). Again, as the cooling rates decrease the amount of the Laves phase that precipitates increases, resulting in deterioration in the impact strength. Therefore, comparing the curves for 850 and 950 °C annealing in Figure 6.18, it can be concluded that grain size plays a measurable role in the nucleation of the Laves phase, as already stated above. The results of this study on the effect of cooling rate on the Charpy impact toughness of ferritic stainless steels, therefore, largely agree with the work of other researchers [7,8,99], i.e. with the cooling rate having a pronounced influence on the impact energy transition of low interstitial ferritic stainless steels, with the lower cooling rates showing a higher transition temperature.

9.4 Recrystallisation and Grain Growth

Although grain growth experienced in this alloy at annealing temperatures above 850°C is generally expected, the “sudden” significant increase in grain size by about 60% within the temperature region 950 to 1000 °C cannot be readily explained by normal grain growth theories and needs some discussion. The most obvious explanation of “grain boundary particle unpinning by dissolution” in this temperature range is the immediate and obvious candidate. Particles that had nucleated on the recrystallisation front may impede the motion of the grain boundary due to Zener drag [142,143]. The resulting retarding force Δp_{ppt} exercised by these particles on the grain boundary is given by:

$$\Delta p_{ppt} = \left(\frac{3}{4}\gamma\right)\left(\frac{V_v}{r}\right) \qquad \text{Equation 9.9}$$

where γ = grain boundary free energy, V_v = volume fraction of the precipitates and r = radius of the precipitate. Note that a significant retarding force is only achieved with a

large volume fraction and small particles. At 850 °C the retarding force may have a relatively small estimated value of ~2 x 10^4 J/m^3 (i.e. small volume fraction and large radius of the Laves phase) and a condition will not easily be reached where it effectively blocks firstly, full recrystallisation and subsequently grain growth to a large degree. A number of authors [143,144,] however, have proposed and observed an alternative process of "continuous recrystallisation" in aluminium alloys in which particles occupy mainly subgrain boundaries and these only become "released" after some coarsening of the particles, where after "full recrystallisation" appears to have occurred in a gradual process. That such a "continuous recrystallisation" process may have occurred also here is quite possible if the TEM microstructures after annealing at 850 and 900°C are compared with each other in Figure 9.8 (a) and (b). After annealing at 850°C subgrains are still very much present and are heavily decorated by the last remnants of the Laves phase while at 900°C, the subgrain boundaries have completely disappeared and the grain boundaries are clean of any Laves or other phases. The effective rate of continuous recrystallisation is, therefore, determined by the rate of coarsening (which is accompanied by the rate of disappearance of the smaller particles), of the Laves phase particles. At 850 °C, recovery has taken place but no recrystallisation while at 900 °C where full recrystallisation has taken place. This shows that at 850 °C, the last remnants of the Laves phase particles are still effective in locking subgrain boundaries but not at 900 °C. Therefore, it cannot be concluded that the sudden increase in grain size at the higher temperature of between 950 °C and 1000 °C was due to an unpinning effect of the grain boundaries by the Laves phase, which had already taken place earlier between 850 and 900 °C.

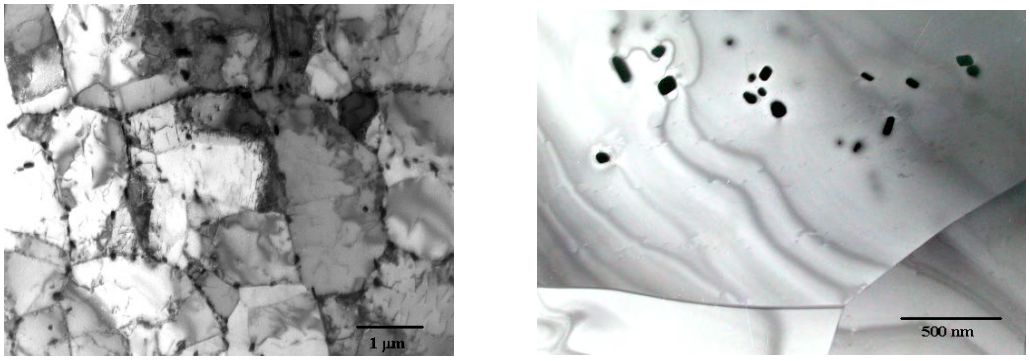

(a) (b)

Figure 9.8. TEM micrographs of the microstructures of the specimens from Steel A that were annealed at (a) 850 °C and (b) 900 °C. Note that with the specimen that was annealed at 900 °C, there were no grain boundary Laves phase precipitates.

An alternative reasoning of "Nb solute drag of sub- and grain boundaries" may be considered in explaining this "sudden" 60% increase in grain size at annealing temperatures between 950 and 1000 °C.

The rate of movement v_b of a recrystallisation boundary in austenite is given by $v_b = p_d M_b$, where p_d is the driving force for recrystallisation and M_b is the boundary's mobility [145]. An increase in recrystallisation rate and subsequent grain growth may, therefore, result either from an increase in the driving force p_d or the mobility M_b of the moving sub- or grain boundary. The quantitative theory of the solute drag effect on a moving grain boundary during recrystallisation was originally formulated by Lücke and Detert [59]. It was later modified by Cahn [60] and then by Lücke and Stüwe [61]. Since then, this theory has been further refined by several authors [57,58,62]. The equation proposed by Cahn on the rate of grain boundary movement as it is affected by solute drag is [63,64]:

$$\frac{p_d}{v_b} = \frac{1}{M_T} = \frac{1}{M_0} + \frac{\alpha X_s}{(1+\beta^2 v_b^2)} \qquad \text{Equation 9.10}$$

where p_d and v_b are defined as above, M_T is the overall mobility due to *intrinsic plus solute drag*, M_0 is the intrinsic grain boundary mobility in pure material, X_s is the atom concentration of solute in the bulk metal, α is a term related to the binding energy of solute to the grain boundary and β is a term related to the diffusion rate of the solute near the grain boundary. The product (αX_s) primarily governs the overall mobility M_T because $(1+\beta^2 v_b^2) > 1$, while if $(1+\beta^2 v_b^2) >> 1$, then $M_T \approx M_0$ and no solute drag occurs. The apparent mobility factor M_T is critically dependent on the binding energy factor α of solute to the boundary and the solute concentration X_s in the bulk metal. The possibility needs to be considered that a fundamental change from "*solute plus intrinsic drag by Nb atoms*" (i.e. controlled by the overall mobility parameter M_T) to one of only "*intrinsic drag*" and now controlled only by the mobility parameter M_0, may occur within the temperature range 950 to 1000°C in this alloy. The question, however, immediately then arises whether such a transition from "solute plus intrinsic drag" at lower temperatures to one of only "intrinsic drag" at about 950 to 1000 °C would not rather be a gradual one than a "sudden" one? That such a "sudden" departure from solute plus intrinsic drag to only intrinsic drag occurs "suddenly" at critical concentrations of the solute or at critical temperatures, has indeed been found by some authors [58].

Firstly, that such a sharp "break" in the effect of low level concentrations of solute in solute drag on grain boundaries (such as the Nb in solution in this alloy) is to be expected, was shown by Suehiro [57]. The author had investigated the effect of temperature on solute drag during recrystallisation in an Fe-Nb alloy. The theoretical analysis predicted that small Nb-additions to iron would reveal a two orders of magnitude sudden decrease in the grain boundary velocity v_b at 700ºC at a critical Nb concentration of 0.15 %wt and this depends on the temperature and total driving force. This retardation was found to be caused by the solute drag effect of Nb on grain boundaries. In further work by Suehiro et al. [58], the author studied the effect of Nb on the austenite to ferrite transformation in an ultra low carbon steel. Their results indicate that there is a critical temperature where the rate of transformation changes drastically. The transformation that occurs above and below the critical temperature are both partitionless massive transformations. The critical temperature was found to be composition dependent, and for the 0.25% Nb alloy it was found to be 760 °C and for 0.75%Nb alloy it was 720 °C. This is in line with the earlier conclusion that the overall mobility parameter M_T is critically dependent on the binding energy α of the solute to the grain boundary. This segregation energy of solute to a grain boundary actually determines the critical concentration of solute at which the mode of recrystallisation may change from interfacial mobility control (or M_0) to one of solute drag (or M_B).
Secondly, the analysis by Le Gall and Jonas [63] of solute drag by sulphur atoms in pure nickel also showed that this transition from solute plus intrinsic drag to purely intrinsic mobility of a grain boundary is not a gradual one but occurs at a critical temperature that provides a "break" in the mobility versus inverse temperature relationship. Furthermore, this critical transition temperature was found to be highly dependent on the concentration of the "dragging" sulphur atoms in solution [64] and may, therefore, vary with different Nb concentrations in solution which, in turn, will be determined by the alloy content and/or by the heat treatments that have led to the Nb in solution.

Although the likelihood that solute drag by Nb atoms was responsible for the sudden increase in grain size between 950 and 1000 °C, could of course, not be fully proven in this study, it remains currently as the only plausible mechanism. The possibility of Nb solute drag affecting the full recrystallisation and later grain growth of type 441 stainless steels may, therefore, be a useful avenue of further study to confirm the above possibility of solute drag being responsible for the "sudden" 60% increase in grain size at about 950 to 1000 °C in this alloy.

CHAPTER TEN

DISCUSSIONS

TRANSFORMATION KINETICS MODELLING

10.1 INTRODUCTION

The purpose of this chapter is to model the transformation kinetics of the Laves phase in AISI type 441 ferritic stainless steel during the isothermal annealing as a typical case. This model takes into account the diffusion of Nb, and is based on the assumption that the precipitation of the Laves phase is the only one taking place. This has been done within the framework of nucleation and growth theory which leads naturally to the coarsening process.

10.2 MODELLING IN KINETICS OF LAVES PHASE PRECIPITATION

10.2.1 NUCLEATION

Classical nucleation theory is used to estimate the nucleation rate for the Laves phase precipitation. There are several formulae for the nucleation rate, for simplicity the general equation for calculating the rate of isothermal heterogeneous nucleation is given by [108]:

$$\dot{N} = \bar{c} N_o \frac{kT}{h} \exp\left(-\frac{\Delta G^* + Q}{RT}\right) \qquad \text{Equation 10.1}$$

$$\Delta G^* = \frac{4\pi\gamma^3 \left\{2 - 3\cos\theta + \cos^3\theta\right\}}{3(\Delta G_v + \Delta G_\varepsilon)^2} \qquad \text{Equation 10.2}$$

where $\bar{c}$ is the amount of Nb additions in the steel, N_o is the number of available nucleation sites, k and h *are* the Boltzmann's and Planck's constants respectively, T is the absolute temperature, ΔG^* is the activation energy for nucleation and γ is the surface energy per unit area of the precipitate – matrix interface. θ is the contact angle between the Laves phase particle and the grain boundary. The critical embryo size r^* for forming a nucleus is given by:

$$r^* = \frac{-4\gamma}{(\Delta G_v + \Delta G_\varepsilon)\left\{2 - \cos\theta - \cos^2\theta\right\}} \qquad \text{Equation 10.3}$$

where ΔG_v is the chemical free energy change per unit volume and ΔG_ε is the misfit strain energy around the particle, which is often relatively small compared to the driving force ΔG_v and, hence, was neglected in the calculations for ΔG^* and r^*.

10.2.2 GROWTH

To simplify this model, it is assumed that all the Laves phase precipitation occurs along the grain boundaries and the growth and nucleation of the precipitates takes place simultaneously as it has often been observed that nucleation is superseded by growth very early within the precipitation process. The growth of the precipitates is assumed to be controlled by the diffusion of the Nb in the ferrite matrix. Assuming that the particle size is large enough for the interface between the precipitate and the matrix to be considered, the position of the interface under one dimensional parabolic growth, which corresponds to the radius of large spherical particles, is given by [5,99,146,147]:

$$r = \Omega\sqrt{D_{Nb}t} \quad \text{with} \quad \Omega \approx \sqrt{2\frac{\bar{c} - c^{\alpha\beta}}{c^{\beta\alpha} - \bar{c}}} \qquad \text{Equation 10.4}$$

where D_{Nb} is the Nb diffusion coefficient in the ferrite matrix, t is the reaction time, Ω is the supersaturation, $\bar{c}$ is the alloying concentration, $c^{\alpha\beta}$ and $c^{\beta\alpha}$ are the equilibrium concentrations in the ferrite matrix α and in the precipitate β (i.e. the Laves phase, Fe_2Nb), respectively. Assuming that $c^{\alpha\beta}$ is approximated to be the solute concentration after ageing for a long period of time and is obtained from the Thermo – Calc® calculations (Table 5.6), the supersaturation of Nb for each steel can be calculated and is shown in Table 10.1.

Table 10.1. Calculated equilibrium mole fractions at the interface Fe_2Nb / ferrite for Nb between 600 and 800 °C in AISI type 441 ferritic stainless steel.

Temperature (°C)	Nb addition (Mole fract.)	Nb in precipitates (Mole fract.)	Nb in solid solution (Mole fract.)	Supersaturation Ω
600	2.83×10^{-3}	2.25×10^{-3}	5.80×10^{-4}	1.410
650		2.00×10^{-3}	8.30×10^{-4}	1.411
700		1.50×10^{-3}	1.33×10^{-3}	1.414
750		1.00×10^{-3}	1.83×10^{-3}	1.416
800		4.20×10^{-4}	2.41×10^{-3}	1.420

From this model, it is further assumed that the nucleation rate $\dot{N}$ for the Laves phase is a constant during precipitation in the ferrite matrix, and that soft – impingement does not occur. At time t the radius of the particle nucleated at time t_1 ($0 < t_1 < t$) is expressed

by Equation 10.6. Assuming a spherical particle, the growth rate G_r at time t_1 is given by:

$$G_r = 4\pi r^2 \frac{dr}{d(t - t_1)} \qquad \text{Equation 10.5}$$

Therefore, the number of nuclei precipitated between t_1 and $t_1 + dt_1$ is $\dot{N}\, dt_1$. The rate of the increase in volume of all the particles formed at t_1 is then given by:

$$\frac{dV}{dt} = \frac{8\sqrt{2}}{3} \pi D_{Nb}^{3/2} \left[\frac{\bar{c} - c^{\alpha\beta}}{c^{\beta\alpha} - \bar{c}} \right]^{\frac{3}{2}} \dot{N}(t - t_1)^{\frac{3}{2}} \qquad \text{Equation 10.6}$$

To convert Equation 10.6 to the volume fraction of the precipitates V_v, this equation is multiplied by $\left(\bar{c} - c^{\alpha\beta}\right) / \left(c^{\beta\alpha} - \bar{c}\right)$. By considering the composition factor and integrating Equation 10.8, the following equation can be obtained [146,147]:

$$V_v = 1 - \exp\left\{ -\frac{16\sqrt{2}}{15} \pi D_{Nb}^{3/2} \left[\frac{\bar{c} - c^{\alpha\beta}}{c^{\alpha\beta} - \bar{c}} \right]^{\frac{1}{2}} \dot{N} t^{\frac{5}{2}} \right\} \qquad \text{Equation 10.7}$$

Equation 10.9 above, is the typical Johnson-Mehl-Avrami-Kolmogorov (*JMAK*) equation applied to describe the kinetics of the single precipitating Laves phase in an AISI type 441 ferritic stainless less and utilising Thermo – Calc® software to predict the driving forces.

10.2.3 COARSENING

The coarsening rate of precipitates can be calculated using the classical theory of the Ostwald ripening equation that is due to Lifshitz and Slyozov [113] and Wagner [114] and is often called LSW coarsening. The LSW coarsening rate equation for diffusion controlled coarsening on a grain boundary is given by:

$$r^4 - r_o^4 = \frac{K_1 \gamma \upsilon^{\beta} D_{gb} c^{\alpha\beta} \delta_{gb}}{kT} t \qquad \text{Equation 10.8}$$

where r is the average particle radius, r_0 the initial average particle radius, γ is the interfacial energy, K_1 is a constant, D_{gb} is the diffusion coefficient down the grain boundary, δ_{gb} is the width of the grain boundary, υ^{β} is the molar volume, T is the absolute temperature and t is the holding time at the isothermal heat treatment temperature. The above coarsening Equation 10.10 is also only fully valid if all of the precipitates were situated on grain boundaries and this is, of course, quite difficult to

achieve. One factor that strongly affects the coarsening stage is the interfacial energy, even though the equilibrium concentration $c^{\alpha\beta}$ is of a primary concern as this may vary by many orders of magnitude from system to system. The coarsening rate is also influenced by the distribution of the particles before the coarsening stage, which is also determined by the nucleation and growth stages. However, in this work there are not enough experimental data to describe quantitatively all of the details of the coarsening process. The specific data that are needed for the further discussion are the changes in the particle size distribution during high temperature ageing.

10.2.4 Diffusion Coefficients

The knowledge of the appropriate diffusion coefficients is required for all the diffusion controlled transformation equations. The overall diffusion coefficient is given by:

$$D = D_o \exp\left(\frac{-Q}{RT}\right) \qquad \text{Equation 10.9}$$

where D_o is the pre-exponent factor, Q is the activation energy for diffusion, R is the gas constant and T is the absolute temperature. Fridberg et al. [148] reported the intrinsic chemical coefficient D_0 for the diffusion of several solutes in a ferritic matrix and that were used in this work, see Table 10.2 below.

Table 10.2 Chemical diffusion coefficients and activation energies of elements in ferrite [after Fridberg et al. 148].

Elements	D_o (m^2s^{-1})	Q ($Jmol^{-1}$)
Cr	1.5×10^{-4}	240×10^3
Mo	1.5×10^{-4}	240×10^3
Nb	1.5×10^{-4}	240×10^3

10.3 Parameters Required for Calculations

The term ΔG_v, the chemical free energy change per unit volume of precipitate, is given by:

$$\Delta G_V = \frac{\Delta G}{\upsilon V_v} \qquad \text{Equation 10.10}$$

where V_v is the equilibrium volume fraction of the Laves phase and υ is the molar volume of the Laves phase, and ΔG is the molar free energy change of the precipitation reaction. ΔG can be obtained with from the thermodynamic calculations using the

Thermo-Calc ® software, see Figure 5.14 and Table 5.6. However, it can also be estimated from the precipitation reaction:

$$[Nb] + 2[Fe] \rightleftharpoons Fe_2Nb \qquad \text{Equation 10.11}$$

where [Nb] and [Fe] are the concentrations in solution in the ferrite. The activity of pure solid Fe_2Nb can be taken to be unity, assuming that the activities of the other elements are equivalent to the concentrations. The solubility product is expressed as the solubility of Nb with the following equation:

$$\ln x_{Nb}^{\alpha\beta} = \frac{A}{T} + B \qquad \text{Equation 10.12}$$

with $A = \frac{\Delta G_o}{R}$ and $B = -\ln[Fe]^2$

and for the driving force ΔG:

$$\Delta G = \Delta G_o - RT \ln x_{Nb}^{\alpha\beta} \qquad \text{Equation 10.13}$$

ΔG can be estimated if the values of A and B are available. $x_{Nb}^{\alpha\beta}$ is the equilibrium mole fraction of Nb in solution in ferrite. Assuming that all of the carbon and nitrogen precipitated as (Ti,Nb)(C,N) and the Fe concentration [Fe] is constant, it is possible to calculate the volume fraction and concentrations in the ferrite at the interface of Nb. Table 10.1 shows the calculated concentrations obtained from the Thermo-Calc® predictions. By plotting the relationship between $\ln x_{Nb}^{\alpha\beta}$ and $1/T$, the constants A, B and ΔG_o in the Equation 10.14 were obtained, as illustrated in Figure 10.1 and the results are given in Table 10.3.

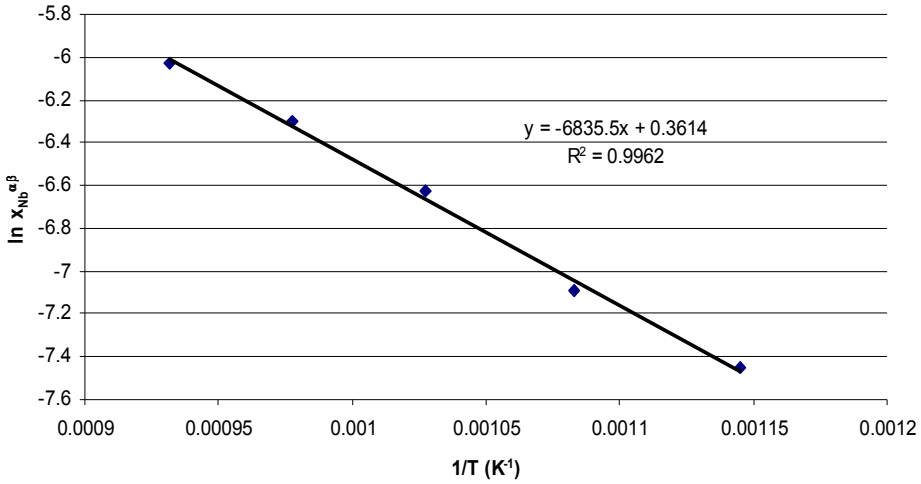

Figure 10.1. The relationship between $\ln x_{Nb}^{\alpha\beta}$ and T^{-1} for AISI type 441 ferritic stainless steel.

Table 10.3. Calculated values of A, B and ΔG_o for Fe_2Nb in AISI type 441 ferritic stainless steel.

	A (K^{-1})	B	ΔG_o ($Jmol^{-1}$)
Values for mole fraction and natural logarithm	-6835.5	0.3614	-56830.35
Values for wt fraction and natural logarithm	-2968.6	0.1569	

The solubility product for the Laves phase Fe_2Nb in the Steel A that was studied here was obtained from Thermo-Calc® calculated data and the experimental data. This expression of the solubility product with weight fraction is given as:

$$\log [Nb] = -2968.6/T + 0.1569 \qquad \text{Equation 10.14}$$

This expression is different from the one obtained by Fujita and co-workers [6] in their recent work. These authors were also working on niobium alloyed ferritic stainless steels, and their expression is as follows:

$$\log [Nb] = -3780.3/T + 2.4646 \qquad \text{Equation 10.15}$$

The thermodynamic expressions for the free energy change ΔG for the precipitation reaction of Laves phase in type 441 ferritic steels were also calculated. This expression with the mole fractions in the ferrite matrix, is given by:

$$\Delta G = -56830.35 - RT\{0.3614 + \ln x_{Nb}^{\alpha\beta}\} \qquad \text{Equation 10.16}$$

From Equation 10.16, it was established that the calculated values for ΔG are about ten times higher than the one obtained by Thermo-Calc® predictions. Therefore, it will be reasonable to rather use the values from the Thermo-Calc® predictions, since they are closer to the values from the literature [117].

10.4 CALCULATIONS

Before the calculations for the Laves phase transformation kinetics can be made, it needs to be noted that the following assumptions were used; (i) no treatment of soft impingement was introduced during the nucleation and growth stage, (ii) the particle – size distribution at different nucleation times and growth rates remained constant and (iii) that the precipitation proceeds in an Fe –Nb –C alloy system. Also, it was assumed that Nb(C,N) does not form, and if it does, its volume fraction will be negligible and, therefore, only the nucleation and growth of Laves phase is taking place. There are two unknown parameters, the number density of nucleation sites N_o and the interfacial energy γ. These parameters are treated as fitting parameters. The calculations were carried out at the two temperatures of 700 and 800 °C. The diffusion coefficient and the activation energy for the diffusion of Nb listed in Table 10.3 were used. The parameters that were used for the Laves phase transformations are shown in Table 10.1.

Table 10.4. Parameters used in the calculations for Laves phase transformation.

Parameters	Values
Boltzmann's constant, h (J/K)	1.38×10^{-23}
Planck's constant, k (Js)	6.626×10^{-34}
Gas constant, R (J/K/mol)	8.314
Avogadro constant, N_A (mol^{-1})	6.022×10^{23}
Unit cell volume, V_{cell} (m^3)	1.57×10^{-28}
Molar volume υ_m for Fe_2Nb (m^3/mol)	2.36×10^{-23}
Density ρ of Fe_2Nb (kg/cm^3)	8.58
Lattice parameter of bcc a_{Fe} (nm)	0.28
Contact angle, θ (°)	24

The activation energy for nucleation ΔG^* and the critical particle size r^* for the Laves phase's nucleation assuming the of the surface energy of the Laves phase γ to be 0.331 Jm^{-2} [5], are shown in Table 10.5 below. It should be noted that both the values of ΔG^* and r^* are dependent on γ , and the values obtained at both temperatures are realistic enough for the particle's nucleation and growth.

Table 10.5. The calculated values of the activation energy for the nucleation ΔG^*, and the critical particle size r^* for the Laves phase's nucleation at the two temperatures of 700 and 800 °C.

Temp. (°C)	ΔG (J/mol)	ΔG_v (J/mol)	ΔG^* (J)	r* (nm)
700	-325	-1.92×10^{8}	8.28×10^{-18}	29.8
800	-90	-2.30×10^{8}	5.72×10^{-18}	24.7

10.4.1 Volume Fraction and Particle Size

Calculated volume fractions for the Laves phase during isothermal annealing at 700 and 800 °C are shown in Figure 10.2 and Figure 10.3 respectively, and compared with the respective experimental observations. The results also show the calculated mean particle's radius with time, but there are no experimental values for comparison. One of the draw backs of this approach is that it does not show an actual estimate of the volume fraction within the steel, i.e the calculations show only the accumulated volume fraction of the Laves phase during the transformation kinetics. Therefore, for comparison purposes the experimental values had to be normalised with respect to their equilibrium volume fraction.

Figure 10.2 shows a similar comparison of the experimental and calculated values for the change of volume fraction and the mean particle radius with time at 700 °C, using reasonable values of $N_o = 4.3 \times 10^{14}$ m^{-3} and $\gamma = 0.331$ Jm^{-2}. However, at 800 °C the calculated results estimated that there are now ten time lower initial nucleation sites for Laves phase than at 700 °C, that is $N_o = 2.9 \times 10^{13}$ m^{-3} and $\gamma = 0.331$ Jm^{-2}. This resulted in lowering the transformation kinetics of the Laves phase nucleation at 800 °C, while the particle's growth rate at 800 °C is much higher than at 700 °C, and this is related to a higher diffusivity of the Nb. Accordingly, a large particle, which has nucleated within the early stages of precipitation, grows continuously even while the volume fraction approaches equilibrium. Because of the capillarity effect, the small particles which nucleated late begin to dissolve from coarsening even though the large one continues to coarsen. It has been demonstrated in the past that the mean particle radius at first increases approximately parabolically with time as all the particles grow from solid solution [105]. The mean radius changes at a rate of about $t^{\frac{1}{3}}$ at longer times as the number density of the particles decreases, and this is consistent with expectations from coarsening theory.

When the experimentally determined activation energy (that is, Q = 211 kJ/mol within the temperature range of 750 to 825 °C) for the Laves phase transformation kinetics is employed in the model, this gives the initial nucleation site density N_o approximately 4.95 x 10^9 m^{-3} at 800 °C.

The sensitivity of the number density of the nucleation sites N_o and the interfacial energy γ has been established in the niobium – alloyed ferritic stainless steel also for M_6C carbides by Fujita et al [5] and it was observed that the results are affected more by the interfacial energy than by the number density. As an example, it was found that an order of magnitude increase in N_o will lead to about a 20% decrease in mean particle size and a corresponding increase in γ will lead to about a three fold increase in mean particle size [5]. The parameters in this work were chosen as fitting parameters to obtain a reasonable agreement with the experimental results.

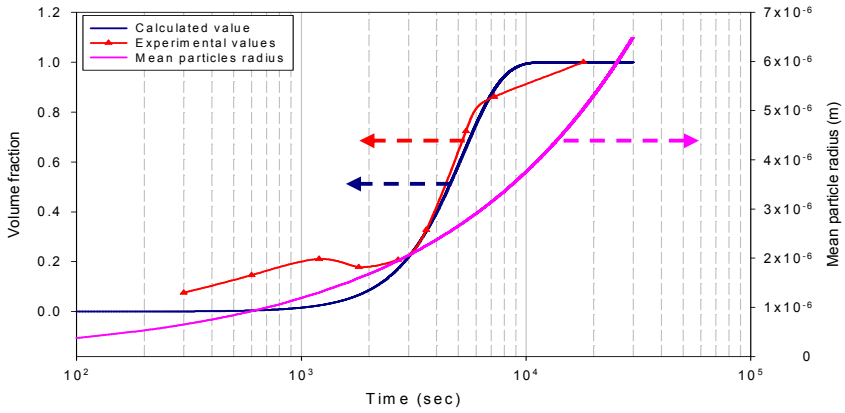

Figure 10.2. Comparison between the experimental data and calculated isothermal transformation curves for the Laves phase's precipitation at 700 °C in the AISI type 441 ferritic stainless, with N_o = 4.3 x 10^{14} m^{-3} and γ = 0.331 Jm^{-2}.

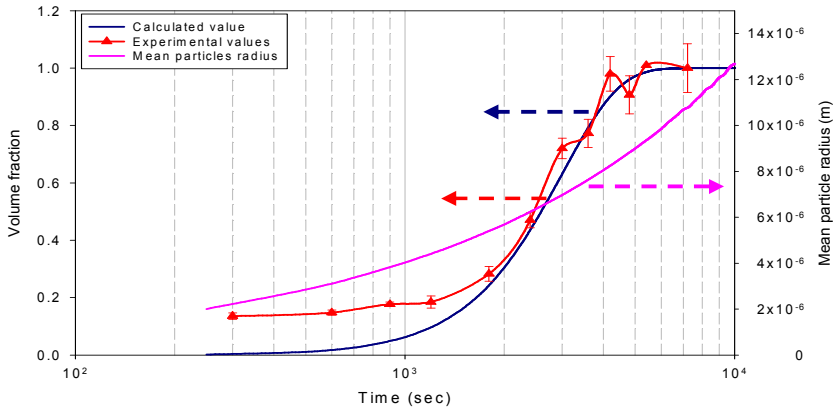

Figure 10.3. Comparison between the experimental data and calculated isothermal transformation curves for the Laves phase precipitation at 800 °C in the AISI type 441 ferritic stainless, with N_o = 2.9 x 10^{13} m^{-3} and γ = 0.331 Jm^{-2}.

10.5 SUMMARY

This model agrees reasonably well with the experimental results and analyses of the microstructures and also qualitatively with the basis of the classical heterogeneous nucleation theory. For instance, it demonstrates that nucleation of the Laves phase on grain boundaries (where the initial nucleation site density N_0 is relatively much lower than for homogeneous nucleation), is dominant at the higher annealing temperatures of 800 °C and above, where the undercooling ΔT and hence the driving forces ΔG_v for nucleation are relatively low and the system then lowers its retarding forces through grain boundary nucleation. As the temperature is decreased and the undercooling ΔT and hence the driving forces are higher, however, heterogeneous nucleation on dislocations becomes more significant, and hence, the initial number of the nucleation sites N_0 becomes higher. The initial number of nucleation sites N_o has a significant impact on the transformation kinetics of the Laves phase, any increase in it results in a decrease in the transformation kinetics, i.e. note the lower value in Figure 10.2 and 10.3 for $t_{50\%}$ at 800°C with N_0 = 2.9x10^{13} m^{-3} if compared to the higher value for $t_{50\%}$ at 700°C with N_0 = 4.3x$10^{14}$$m^{-3}$.

CHAPTER ELEVEN

CONCLUSIONS AND SUGGESTIONS FOR FURTHER WORK

11.1 CONCLUSIONS

The effects of some metallurgical and mechanical factors on the Charpy impact toughness of AISI type 441 have been investigated. The following may be concluded:

- The steel has an acceptable impact toughness of approximately 60 J after being solution annealed at 850°C while below or above this heat treatment the impact toughness decreases significantly, falling to values as low as only 10 J. At temperatures above 850 °C grain growth plays a dominant role in lowering the impact toughness, but at temperatures below 850 °C, the low impact toughness is associated with the precipitation of the intermetallic Laves phase on grain boundaries. The results of the effect of annealing temperature on the Laves phase precipitation agrees with the prediction made by Thermo – Calc®, whereby an increase in Laves phase volume fraction resulted in lowering of the room temperature impact toughness of this AISI type 441 ferritic stainless steel.

- When comparing the results for Steel A from the Thermo-Calc® predictions and the experimental values, Thermo-Calc® predicts that at 825 °C, the weight fraction of the Laves phase should be zero, whereas the experimental results prove that there is still about 0.031wt% of Laves phase present and this remnant still exists even up at 850 °C and above.

- Also, the Thermo-Calc® predictions and the experimental results show that the volume fraction, the solvus temperature and the composition of the precipitates are dependent on the composition of the steel. The stoichiometric composition, also changes with the annealing temperatures.

- The ductile – to – brittle transition temperature (DBTT) is dependent on both the grain size and the presence of Laves phase precipitates on grain boundaries, but the upper shelf energy appears to be only dependent on the presence of the Laves phase precipitates. When a Cottrell approach was used to model the effect of grain size on the embrittllement of the Steel A, it was observed that according to the model, that at temperatures above and below 850 °C the steel

will still be brittle. Therefore, it cannot be confidentially assumed that at temperatures below 850 °C, the grain size plays a significant role in embrittling this steel. It was also observed that over the range of grain size from 25.2 to 55.9 µm in Steel A, there is a positive shift of 35 °C in the transition temperature. It was found that this sensitivity of the DBTT on grain size can be lowered by increasing the alloy content of the steel, making it less pure (such as in Steels C to E).

- When applying the Smith model of brittle grain boundary carbides on the embrittlement of Steel A, the predicted outcome and the experimental results do not agree quantitatively although qualitatively some resemblance between what is predicted and what was found was observed. For instance, the width C_o of the embrittling second phase is related, firstly, to the volume fraction V_v of the Laves phase but also secondly, to the grain size, the latter through the grain boundary nucleation site concentration with a larger sub- and grain size leading to a thicker C_o through less available Laves phase nucleation sites. Therefore, both a higher volume fraction as well as a larger sub- and grain size will then decrease the effective fracture stress of the steel though a higher value of C_o. Due to the low volume fractions of the (Ti,Nb)(C,N) and M_6C type Fe_3Nb_3C carbides, it was concluded that they don't have any significance in the embrittllement in these steels. In this case, for any given volume fraction of the (Ti,Nb)(C,N) precipitates, the effective surface energy of the crack γ_f will be higher for a distribution within the grain's interior. Therefore, the possibilities of transgranular or cleavage fracture occurring are minimised.

- The cooling rate has a pronounced influence on the severity of the Laves phase embrittlement of these steels after annealing at 850 °C. After cooling from 950 °C with an already embrittled structure from grain growth, the introduction of Laves phase during slow cooling does not introduce a significant and measurable additional embrittlement. In steels of this type, the embrittlement caused by excessive grain growth is, therefore, overriding.

- Annealing at temperatures above 850 °C in this alloy, generally expected grain growth was experienced, but, there was a "sudden" significant increase in grain size of about 60% within the temperature region 950 to 1000 °C. As no grain boundary pinning was evident at these temperatures, it was postulated that Nb

solute drag may be responsible for this "sudden release" of the grain boundaries, affecting the full recrystallisation and later grain growth of type 441 stainless steels at lower temperatures.

On the transformation kinetics of the Laves phase precipitates, the following could be concluded:

- A time – temperature – precipitation (*TTP*) diagram for the Laves phase that was determined from the transformation kinetic curves appears to show two classical C noses on the transformation curves, i.e. the first one occurring at higher temperatures of about 750 to 825 °C and the second one at much lower temperatures, estimated to possibly be in the range of about 650 to 675 °C. The transmission electron microscopy (TEM) analyses show that there are two independent nucleation mechanisms that are occurring at these temperatures. At the lower temperatures of about 600 °C, the pertaining nucleation mechanism is principally on dislocations and as the temperature is increased to above 750 °C, grain boundary nucleation becomes more dominant.
- The effects of grain size and Mo additions on the transformation kinetics of the Laves phase, showed that, by increasing the grain size or adding the alloying element Mo, that these lower the rate of formation of the Laves phase.
- By assuming an interfacial energy of 0.331 Jm^{-2} for the Laves phase, the kinetic model predicts that at 700 °C and 800 °C the initial number of nucleation sites N_o is 4.3 x 10^{14} m^{-3} and 2.9 x 10^{13} m^{-3}, respectively. These parameters fit well with the experimental results. When the experimentally determined activation energy of Q = 211 kJ/mol for the Laves phase transformation kinetics is employed in the model, this gives the initial nucleation site density N_o approximately as 4.95 x 10^{9} m^{-3} at 800 °C, indicating that there might be fewer nucleation sites than expected. This would agree well with heterogeneous nucleation on grain boundaries with a much lower nucleation site density instead of homogeneous nucleation.
- The solubility products of the Laves phase Fe_2Nb in the AISI type 441 ferritic stainless steel obtained from Thermo-Calc® calculated data and the experimental data, is given as:

$$\log [Nb] = -2968.6/T + 0.1569$$

11.2 SUGGESTIONS FOR THE FURTHER WORK

The effect of the steel's composition on the toughness of AISI type 441 ferritic stainless steel still needs to explored further, especially the optimum Mo content that is required to lower both the solvus temperature and the volume fraction of the Laves phase precipitation. Also, the minimum Nb content that will be optimum to stabilise the type 441 ferritic stainless steels, whilst at the same time providing the desired heat resistant properties, and lowering the Laves phase content, also needs to be investigated further.

The possibility of Nb solute drag affecting the full recrystallisation and later grain growth of type 441 stainless steels will be a useful avenue of further study to confirm possibility of the disappearance of Nb solute drag being responsible for the "sudden" 60% increase in grain size at about 950 to 1000 °C in this alloy.

Validation of the modelling of the transformation kinetics for the Laves phase that will improve the precision of any predictions in future:

1. specific characteristics of the nucleation sites;
2. measurement of the interfacial energy; and
3. modelling of precipitation on grain boundaries.